29th European Photovoltaic Solar Energy Conference and Exhibition,
Amsterdam, the Netherlands, 22-26 September 2014

THE BIPV RESEARCH FACILITY 'SOLARBEAT' IN THE NETHERLANDS

R.M.E. Valckenborg[1]*, A. de Vries[2], W. Folkerts[1] and G.P.J. Verbong[3]
[1] Solar Energy Application Centre (SEAC), High Tech Campus 21, NL-5656 AE Eindhoven, The Netherlands
[2] Holland Solar, Korte Elisabethstraat 6, NL-3511 JG Utrecht, The Netherlands
[3] TU/e EEI office, CNT 1.15b, PO Box 513, NL-5600 MB Eindhoven, The Netherlands
*Corresponding author: valckenborg@seac.cc; Tel: +31 652803729

ABSTRACT: A BIPV research facility 'SolarBEAT' has been initiated in the Netherlands by the Solar Energy Application Centre (SEAC). This facility enables and supports research and development of new products in the field of BIPV, solar thermal and PVT. Projects are carried out by consortia in which research institutes and companies work together. The SolarBEAT facility is a cooperation between SEAC, the branch organization Holland Solar and the TU Eindhoven and is located on a large south oriented roof with a clean horizon. The roof is equipped with a variety of high quality sensors and measurement equipment in order to enable research projects on BIPV and PVT in a realistic outdoor setting. IR-thermography and outdoor Electroluminescence (EL) are developed for thermal research and reliability and durability monitoring over longer periods. We define three new effective ways of analyzing results, which can and will be applied to all BIPV-prototypes. They are an irradiance stamp plot (figure 6), thermal stamp plot (figure 9) and integrated-NOCT plot (figure 10). The performance of the first project in SolarBEAT can be understood quite well by comparing it to the thermal model that we have developed for BIPV-products. The quantitative heating up of the various panels as a function of air gap width, position in the setup, and weather conditions can be understood.

1 INTRODUCTION

Photovoltaic plays an important role in the National Renewable Energy Action Plans of many European countries. An important reason for this is that PV is one of the few suitable technologies for decentralized renewable energy production in an urban environment. Between 2007 and 2013 the price of standard PV modules declined by 75%. This enables the use of low cost PV laminates as a starting point for a largely diversified BIPV market. Added value of BIPV is realized by improved aesthetics and by multi-functional application of BIPV in the building skin. Increased attention for BIPV in the Netherlands has also lead to a dedicated norm NEN 7250 'Solar energy systems - Integration in roofs and facades - Building aspects' [1], which is probably going to serve as a basis for a European version.

To our opinion, the main research topics on BIPV(T) can be summarized as:

- Performance of BIPV, to be understood in a performance (yield) model that incorporates all relevant environmental parameters and boundary conditions, like irradiation, orientation, ambient temperature, partial shading situation, etc.
- Design of the various BIPV products, like design of back ventilation to prevent excessive heat-up. And the BIPV functionality as a building material in a cost-effective way.
- Use of alternative materials in BIPV with building code compliant materials, and non-glass materials.
- BIPV system design, including repair and maintenance aspects, 'plug-and-play' design, and prevention of power loss from shading and pollution.
- Architectural aspects of BIPV, like aesthetics, and full flexibility in color, shape and size.

To address al these topics, the SolarBEAT facility has been initiated early 2014. It is an outdoor Research & Development infrastructure for new BIPV- and PVT-products. This facility is a cooperation between SEAC, Holland Solar and the TU Eindhoven. Project partners that are using SolarBEAT come from institutes, small & medium enterprises (SME) and multinationals. Most of them work in the field of solar energy or building physics. Especially fruitful are project consortiums which are a balanced mixture with partners from both fields. Other stakeholders of SolarBEAT are real estate developers and architects, that can benefit from the demonstrated prototypes, and adapt them into their own plans. In this paper we present the SolarBEAT infrastructure to the solar community, and discuss some of the major topics of research which are mentioned above.

2 SOLARBEAT INFRASTRUCTURE

2.1 Dummy houses/attics

SolarBEAT is located on a large south oriented roof with a clean horizon. The roof is equipped with a variety of high quality sensors and measurement equipment in order to investigate all key topics of BIPV(T) research in a realistic outdoor setting.

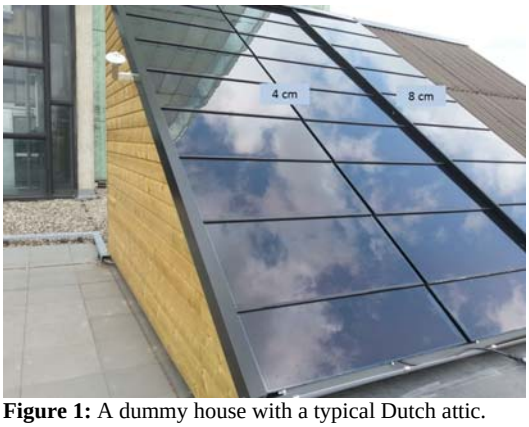

Figure 1: A dummy house with a typical Dutch attic. Three rows are used for experiments with a new BIPV-product that is combining thermal insulation and CdTe PV-panels. The insets shows the air gap depth, which is varied between 4 and 8 cm to investigate thermal effects.

The SolarBEAT facility can accommodate six independent projects which each have their own attic to carry out experiments. The attics have a dimension of 6m x 5m floor print, and a tilt angle of 35°. See figure 1 for an example. Mutual shading is limited to a minimum. Each project has a clean horizon for 99% of the time, as has been measured with the Solmetric SunEye fish-eye camera and corresponding software. Every project has a first class pyranometer in the Plane Of Array (POA).

Figure 2: Solar Measurement and Weather Station at SolarBEAT. The green building in the background is in the North.

2.2 Solar Measurement and Meteorological Station

We measure the irradiance by one central installed Solar Measurement Station (SMS), see figure 2. This SMS is equipped with a first class pyrheliometer for the Direct Normal Irradiance (DNI), a secondary standard pyranometer with shading ball for the Diffuse Horizontal Irradiance (DHI), and an unshaded secondary standard pyranometer for the Global Horizontal Irradiance (GHI). The pyrheliometer and shading ball are mounted on a tracker which is following the sun through the sky by a combination of internal calculations and adjustment by measurement. The azimuth and solar zenith are used directly to calculate the extraterrestrial global horizontal irradiance G_0.

The SMS is completed with a meteorological weather station, which is measuring per minute: ambient temperature, averaged wind speed, gust wind speed, wind direction, dew point, pressure, relative humidity, and precipitation (both rain and snow). These parameters are used to study the influence of weather on the performance.

2.3 Sensors and data analysis

For BIPV-product development, it is necessary to measure the building related physics accurately. The air velocity in the ventilation shaft (air gap) behind the PV-panel is measured by hot-wire anemometers. The relative humidity is measured with a capacitive sensor. Temperatures are measured by various methods. A Pt100 thermal resistance is used whenever space allows. In case of limited space (for very small shafts), thermocouples of type T are used. All sensors related to the thermal behavior are monitored per minute. Building parameters are also sampled once per minute, unless for specific cases faster sampling would be needed, e.g. in case of wind gust speed fluctuations. For shading research on the electrical efficiency of inverters or Module Level Power Electronics (MLPE) in general, the default sampling time is once per second. At the moment, we monitor in total 754 sensors producing 13.1 million data points per day. To manage this amount of data, we have designed a dedicated dataflow procedure. Every data logger is uploading the results of the previous day at midnight. Dedicated software is processing this data in a structured way into an SQL-database. During the day, project members can view all data of their own project by a GUI, or by requesting Excel or CSV-files from their own preferred sensors from specific time periods and intervals. Moreover, complex data analysis can be done by a comprehensive mixture of Python-coding and SQL-querying.

Finally, it should be noted that all measurements and reporting are complying with IEC61724 [2]. For specific BIPV-parameters that are not covered by this norm (like e.g. air speed measurements in ventilation shaft) we make use of the most relevant building norm. Table I gives an overview of the most important equipment including accuracy.

Table I: Sensors and measurement equipment.

equipment	brand	type	accuracy
Sun tracker	EKO	Str-22G	
Pyranometer (for GHI)	EKO	MS-802	sec.standard
Shading ball (for DHI)	EKO	MB-12	
Pyrheliometer (for DNI)	EKO	MS-56	first class
Pyranometer (for G_{POA})	EKO	MS-402	first class
Hot-wire anemometer	DeltaOhm	HD2903T	0.06m/s
Pressure sensor	DeltaOhm	HD404T	1 Pa
RH sensor	DeltaOhm	HD4817ET	2%
Temperature sensor	DeltaOhm	HD4817ET	0.3°C
Thermocouples	Roessel	TypeT	1.0°C
Weather station	Lufft	WS600	

2.4 Outdoor IR-thermography

Building integration is crucial for the overall performance of the BIPV-product, and therefore one should perform this analysis outdoor and built-in the roof. Using IR-thermography on the first prototype already provided useful results, both on the overall heat production, as well as on various detailed zoomed areas. Shown in figure 3 is the lower part of a prototype that has two distinctive heated areas, which are caused by the micro-inverters at the back of the panel. The outcome of the thermal model of the complete building element, will make clear if this extra amount of heating by the micro-inverters is acceptable or not.

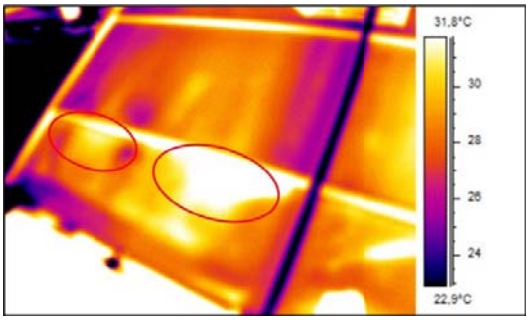

Figure 3: In the lower part of the left element, the two red ellipsis denote the heated areas that are revealed by outdoor IR-thermography.

2.5 Outdoor Electroluminescence (EL)

In (non-destructive) EL-imaging, the PV-panel is operated under forward bias conditions. The current makes the PN-junction work as a LED. This characterization technique takes advantage of the radiative recombination in order to have the possibility to identify defects that are not visible to the human eye. Depending on the band gap of the material, a PV panel will emit photons in a specific wavelength range. These can be made visible on a digital camera (a camera with a CMOS sensor was used in this case) by taking the following measures: shielding the ambient light, taking long enough exposure time (up to a minute) and replacing the original filter with normal glass and adding an IR 850nm filter. It is our ambition to make the EL-technique work for the outdoor situation and for all PV-technologies. In figure 8, one can see the first measurements taken indoors, which show a great potential.

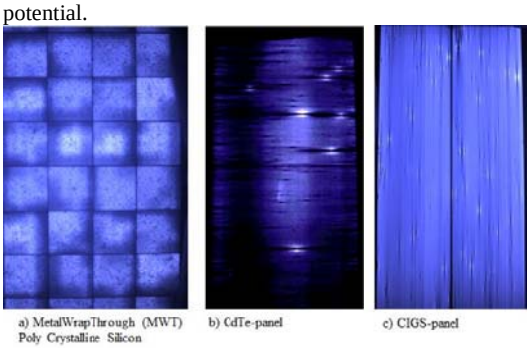

Figure 4: Examples of EL on various technologies (crystalline, CdTe, CIGS) revealing hot spots and other defects on old panels which have been used extensively in experiments.

The defects that can be identified with this technique are: shunt resistances, broken fingers, micro cracks (which can represent a partial or total interruption), furnace belt burns, uneven cell quality, hotspots and black cores. Defects will be different for each material, so not all of the mentioned defect can be found in every PV panel. Some defects can be related to production processes problems, e.g. when patterns can be identified in the same location in different panels/cells this means an error in the manufacturing line. Another cause for these defects is an improper handling of the panels, such as mechanical loads during installation. The samples were taken from previous research and therefore might have more anomalies than panels coming directly from the factory.

3 RESULTS

3.1 Meteorological results

In figure 5 the most important irradiance parameters are plotted for a day with much fluctuations (7th August 2014). This figure shows a completely overcast morning with only diffuse irradiance, followed by brightening just before noon, followed by a sunny afternoon (with some very short cloudy periods) and finally complete overcast at the end of the day.

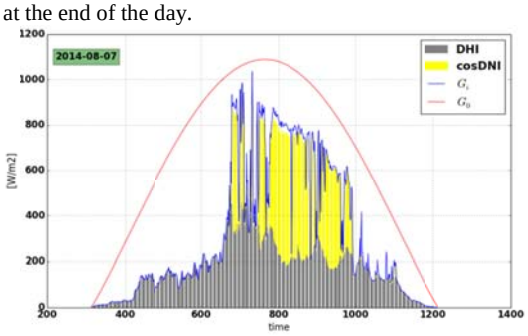

Figure 5: Horizontal irradiance for 7th August 2014 at SolarBEAT. GHI, DHI and (normal component of) DNI are measured. The extraterrestrial irradiance (G_0) is calculated based on measured azimuth and solar zenith angle from the tracker of the SMS.

In order to enable efficient data analysis for the project partners, we adopt the 3 categories (see table II) [3], based on the daily clearness index $k_{T,day}$ as defined by the usual definition of: $k_{T,day}$ = daily sum (GHI) / daily sum (G_0).

Table II: Daily categories based on $k_{T,day.}$

	Lower border	Upper border
Cloudy Day	0	0.20
Fluctuating Overcast Day	0.20	0.60
Sunny Day	0.60	1.0

Also the daily sums of the solar parameters are useful for efficient research. See table III that contains one example day for each category. Moreover, as we measure per minute, we are able to present histograms of e.g. clearness index $k_{T,min}$, which is much more powerful than the widely used daily averaged clearness index $k_{T,day.}$ For a comprehensive overview of the relevant irradiance parameters, we propose to make us of a stamp plot like presented in figure 6. In the histogram we plot the two different ways of aggregating to one single parameter. The red line denotes the usual definition of $k_{T,day}$ like explained above. The yellow line denotes the averaged $<k_{T,min}>$ which is giving a more clean average. Nevertheless, we propose to keep using both parameters, because the classical parameter $k_{T,day}$ is widely used.

Table III: Aggregated irradiance parameters for some example days in July and August.

	18nd July	21st July	2nd Aug.
Extraterrestrial G_0 [kWh/m^2]	11.0	10.9	10.3
GHI [kWh/m^2]	7.5	1.8	4.7
DHI [kWh/m^2]	1.8	1.8	2.8
DNI [kWh/m^2]	9.0	0.0	3.2
$k_{T,day}$ [-]	0.67	0.17	0.45
averaged $< k_{T,min} >$ [-]	0.61	0.14	0.42
typical day [classification]	sunny	cloudy	fluctuating overcast

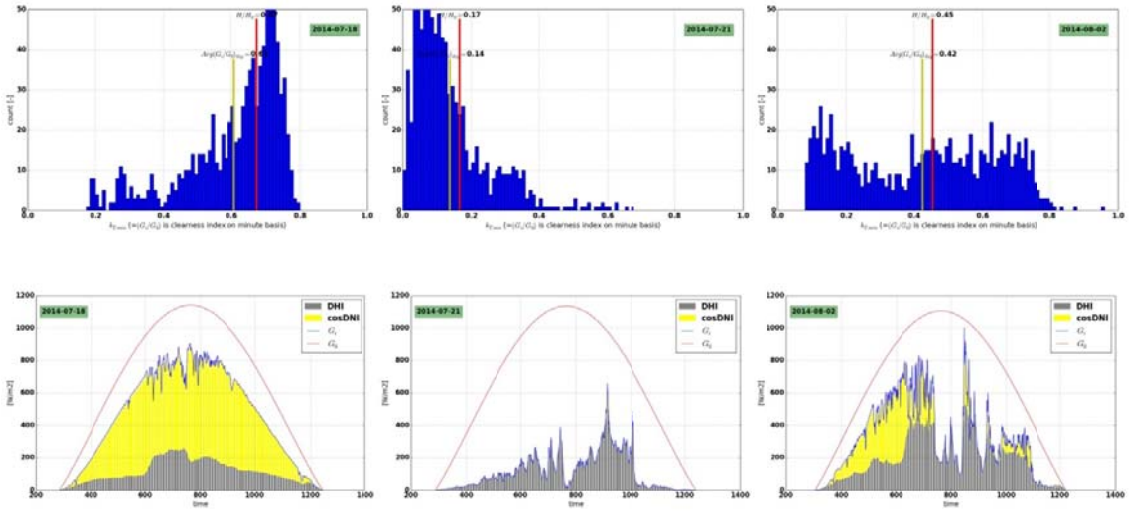

Figure 6: Irradiance Stamp Plot. From left to right: a typical sunny day (18th July), a cloudy day (21st July), and a fluctuating overcast day (2ndAug). Top row: histogram of minutely calculated clearness index. The red vertical line denotes the normal clearness index, which is defined as the daily summed GHI divided by the daily summed extraterrestrial G_0. The yellow vertical line denotes the daily averaged 'clearness index per minute'. Bottom row: GHI, DHI and (normal component of) DNI as measured by the SMS and the extraterrestrial irradiance (G_0).

3.2 Performance measurements and model

The most interesting research goal of SolarBEAT is to develop the performance model for the various projects and prototypes at the facility based on performance measurements. For PV-projects, energy is expressed in AC-power fed-into the grid every minute (24/7). For Solar Thermal (ST) projects, energy is measured by the increased temperature of the cooling liquid that enters the prototype always at a constant temperature. Combined PVT-projects will logically have a combined deliverable on their performance of the PV-part and the ST-part. At the moment of writing, PV-projects are fully functioning and the infrastructure for the ST and PVT-projects is being installed.

The electrical performance can be seen as a chain of efficiencies, see e.g. the IEA PVPS Task 13 report [4], but also shown in many other references [5]. Starting from the input side of solar energy, we measure the irradiance that is captured by a PV-module accurately (as shown in figure 5). The PV-module is converting this irradiance into electrical DC-power which is measured during an IV-sweep. From these IV-curves, measured every minute and for every module, we derive typical DC electrical parameters, see figure 7 for some example curves.

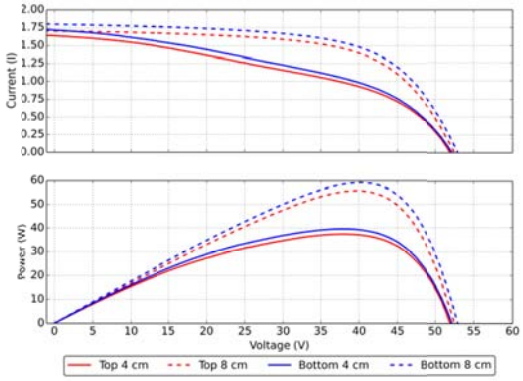

Figure 7a: DC IV-curves and DC **7b:** PV-curves for six panels in the first project on the 23th July.

We read (and fit) the following electrical DC-parameters: V_{OC}, I_{SC}, FF, V_{MPP}, I_{MPP}, P_{MPP}, and η. Because T_{module} and G_{POA} is also measured at the same moment, the STC equivalents are calculated as well. Monitoring these parameters as function of time, or watching fast forward time-lapse movies of these IV-curves reveal anomalies in behavior which could lead to further investigation to the underlying causes (e.g. unexpected shading; bird-droppings; reliability issues).

As a good example of a relevant discovery, figure 7 shows an interesting phenomenon which is very important for the first project in SolarBEAT. The dashed lines show an IV-curve that is corresponding to data of the datasheet of the manufacturer. But the solid lines show a significant lowering in current, and hence also in power at P_{MMP}. By further analysis of the times that this behavior is occurring, we discovered an unwanted shading effect from the ridge and side of the roof. This feedback will lead to a new prototype that will have all PV-panels producing power like the dashed lines in the right plot of figure 7.

All projects in SolarBEAT at the moment convert the

DC-power into AC-power. This can be done by classical inverters on string level, by micro-inverters on panel level or by power optimizers. The efficiency of this step is very susceptible to shading, which can pass relative fast. Therefore this step in the chain of efficiencies is measured on a one second basis. Results are published in a separate paper [6]. The final AC power production (of a specific string) of the prototype is off course an important parameter for the BIPV-product under the specific weather conditions; see figure 8 for an example.

Figure 8: AC power measured per second, possibly averaged in various relevant time scales (1 minute, 5 minute, 1 hour, 1day).

3.3 Thermal measurements and model

It is beyond the scope of this paper to present the complete thermal model that has been developed with the data measured at SolarBEAT. However, we will present the Thermal Stamp Plot that gives us much insight in the performance of the BIPV-product with a focus on the thermal effect. See figure 9. We choose 23th July 2014 (a sunny day with $k_{T,day}$ = 0.68) starting from noon which gives us a nice clean period without any big clouds and any other disturbing shading effects. So all observed effects should and can be explained by our thermal model. We look at four PV-panels in total, two with a ventilation gap of 4 cm (solid lines), and two with a ventilation gap of 8 cm (dashed lines), see figure 1 for a picture of the panels. One can see that in general the top-panels (red lines) perform less than the bottom-panels (blue lines). This can be explained from looking to subplot b which reveals that the top panels will heat up more during a sunny day than the bottom panels. This is caused by the stack effect, which has been described in many articles [7]. However, the effect is smaller than one would expect; we have to zoom to see the more subtle temperature differences. Therefore we present subplot c in which we take the temperature of the hottest panel (top, 4cm) as reference. Two effects are now revealed. Firstly, we observe an average temperature difference of about 3ºC for the 8cm panels (dashed lines). Secondly the average temperature difference between the top and bottom 4cm panel is round 1.5ºC. The logical explanation for this is as follows. The bottom panels (dashed lines) are not that much influenced by the air gap thickness, as they get the same ambient temperature as inlet flow. The stack effect causes panels getting heated up more, when they are further away from the inlet. The larger the air gap, the less stack effect. Hence the 4cm row heats up more than the 8cm row. This corresponds quite well with simulations done with our thermal model (in TRNSYS Type 566). The quality of our thermal model at the moment is on the order of 3ºC RMSE between measurement and model. This model predicts the observed small differences only for largely blocked airflows. By looking to these temperature measurements on such a detailed level, we have learned that the precise design of the BIPV-ventilation channel is crucial for the thermal behavior. And indeed the airflow appears to be blocked too much in the current version of the prototype. Therefore a new version prototype will focus much more on a free airflow in the ventilation shaft. Also a prototype version with a forced airflow is now under consideration.

In conclusion, we like to define the Thermal Stamp Plot as figure 9, to be the default way of an efficient analysis of thermal effects. It serves a twofold goal. On the one hand, it enables us to continuously improve our thermal model of BIPV-products. On the other hand, it leads very fast to a next generation BIPV-prototype.

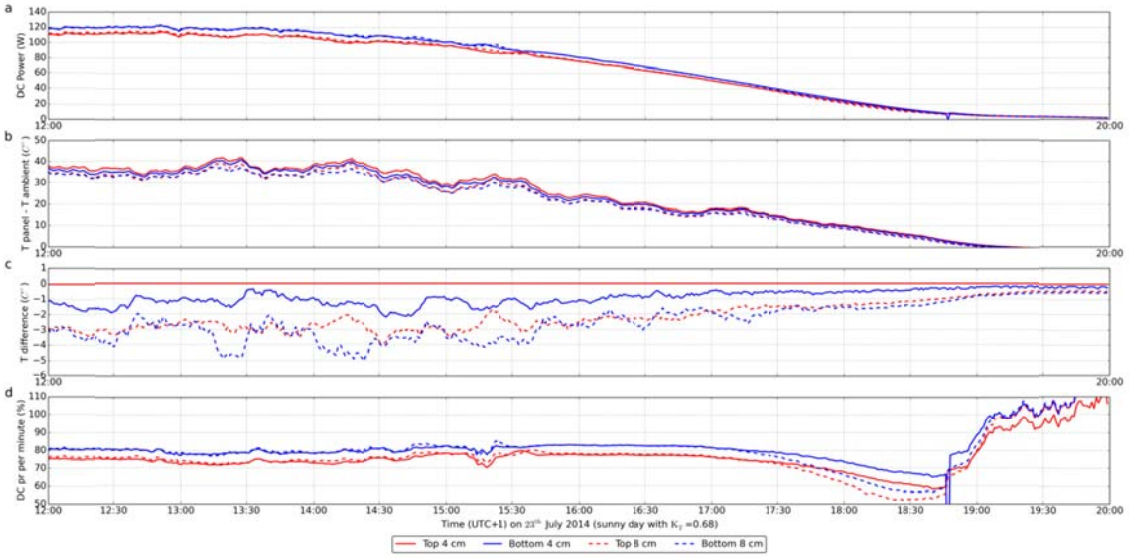

Figure 9: Thermal Stamp Plot. Example plot for first BIPV-project in SolarBEAT. As a function of time of the day are presented: a) DC power. b) Temperature difference between panel and ambient. c) Taking the hottest panel as reference for the other panels. d) minutely calculated DC performance ratio (%).

3.4 integrated-NOCT

As required by IEC61215 [8], a solar panel manufacturer is obliged to publish the Nominal Operating Cell Temperature (NOCT) in the data sheet. This gives a fair estimate of the temperature reached by the panel in an open rack installation under a standard reference condition ($G=800W/m^2$, $S_w=1$ m/s, $T_{amb}=20^oC$). However, BIPV-products are never installed in an open rack. Therefore their temperature will be higher than the NOCT. Not much is known about how much higher quantitatively, sometimes giving room for speculations of poor performance of BIPV in general. This urban legend can be demystified by publishing an i-NOCT which has the same definition and procedure as the normal NOCT, with one exception that the product is measured as it is integrated in the roof as it should be according to the manufacturer and done by an experienced installer. In figure 10, an example is shown of the difference between module and ambient temperature T_{mod}-T_{amb} as a function of in-plane horizontal irradiance G_{POA} for the 4cm and 8cm row on the 23th July. We can read the i-NOCT at $G=800$ W/m^2 (and adding $T_{amb}=20^oC$ by definition from the norm) to be 56°C for the top 4cm panel and 53°C for the bottom 8cm panel. This difference can be understood from our thermal model and by the observation that top panels are hotter than bottom panels, and 4cm panels are hotter than 8cm panels. Normal NOCT values are around 45°C (not shown in this paper). Hence the hottest panel in the test field is 11°C above NOCT for the BIPV-application. This corresponds for CdTe-technology to a performance loss of about 3% relative. It is up to the client to decide whether this balances with the improved aesthetics, but it appears to be quite acceptable to us.

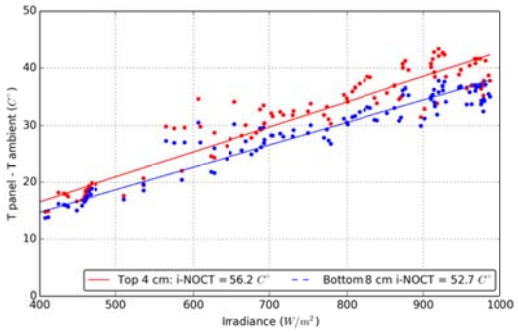

Figure 10: Example of measurement of T_{panel}-T_{amb} as a function of G_{POA} for determining the i-NOCT for the hottest panel (top, 4cm, red data) and coolest panel (bottom, 8cm, blue data) in the setup.

4 CONCLUSIONS

This year the Dutch SolarBEAT outdoor research facility has started successfully with BIPV-project partners that are developing and improving their prototypes at the moment. The infrastructure is ready for hosting six independent PV-projects, all with a clean horizon for 99% of the time. Half of these positions are equipped with a cooling liquid connection to allow for research on ST and PVT-prototypes.

A secondary standard solar measurement station is up and running for several months and producing the following irradiance parameters: G_0, solar azimuth and zenith angles, GHI, DHI, DNI, and $k_{T,min}$ on a one minute time basis, and very reliable (not missing a single minute yet). This one minute time basis enables us to calculate clearness index per minute and present a complete histogram per day. These histograms are a good addition to the usual irradiance parameters, and can reveal substantial periods of clear sky, which are easily obscured in the average value. We define an Irradiance Stamp Plot with a layout as shown in figure 6, as a powerful analysis tool for all projects in SolarBEAT.

The thermal performance is very important for BIPV as one would expect higher panel temperatures due to building integration. By using the example of the first project in SolarBEAT (see figure 1) in which the air gap depth is varied between 4cm and 8cm, we can demonstrate the different thermal behavior of the panels. Moreover, we revealed that the temperature difference is smaller than our thermal model predicts. And therefore we can conclude that the air flow is blocked too much if one would like to benefit from the air gap in its full possibility. Finally, we define a Thermal Stamp Plot with a layout as shown in figure 9, as a powerful analysis tool for all projects in SolarBEAT.

The electrical performance of BIPV-prototypes is analyzed on a detailed level revealing the efficiency of every step in the total chain. First a reliable measurement of incoming solar irradiation. Secondly the DC-power produced by every panel. Third the final AC-power as fed into the grid. Every step is done on a one-minute basis for sunlight hours, unless a higher measurement frequency is required (e.g. for shading effects on the AC-power production of MLPE). We define an i-NOCT plot with a layout as shown in figure 10 as the building integrated analogy of the commonly used NOCT-plot. It gives a more honest prediction of built-in panel temperature, and shows that heating up can be limited by taking care of ventilation effects during product development.

Two important analysis techniques for reliability issues are IR-thermography and Electroluminescence (EL). Both are used in the outdoor situation. For IR, this is a more or less default technique, nevertheless powerful and revealing unexpected heating up. For EL, some development of the measurement equipment itself is being done at the moment.

5 REFERENCES

[1] NEN 7250:2014 ‘Solar energy systems - Integration in roofs and facades - Building aspects’
[2] IEC61724:1998, ‘Photovoltaic system performance monitoring Guidelines for measurement, data exchange and analysis’
[3] D.T. Reindl, W.A. Beckman, and J.A. Duffie, ‘Diffuse Fraction Correlations’, Solar Energy Vol. 45 (1990), No.1, pp.1-7
[4] IEA PVPS Task 13, ‘Analytical Monitoring of Grid-connected Photovoltaic Systems, Good Practices for Monitoring and Performance Analysis’, Subtask 2 Report IEA-PVPS T13-03:2014, March 2014
[5] Woyte A., Richter M., Moser D., Mau S., Reich M. Jahn U., 'Monitoring of Photovoltaic systems: good practices and systematic analysis', Proc. 28th European PVSEC 2013
[6] S. Sinapis, G. Litjens, M. van den Donker, W. Folkerts, ‘Outdoor Characterization of three PV

Architectures under Clear and Shaded Conditions', 5AO.9.6, Proc. 29th European PVSEC 2014
[7] M. Smith, A. Miller, Proceedings 17th European Photovoltaic Solar Energy Conference, Vol. I (2002) 903.
[8] IEC61215:2005, 'Crystalline silicon terrestrial photovoltaic (PV) modules – Design qualification and type approval'

6 ACKNOWLEDGEMENT

This work is supported by 'Rijksdienst voor Ondernemend Nederland' (RVO) and the Dutch Topteam Energy via the project: 'Solar Building Elements Application Test Garden (SolarBEAT)' with grant number TKIZ01018.